JACS
JOURNAL OF THE AMERICAN CHEMICAL SOCIETY
Communication
pubs.acs.org/JACS

Redox-Active On-Surface Assembly of Metal–Organic Chains with Single-Site Pt(II)

Daniel Skomski, Christopher D. Tempas, Kevin A. Smith, and Steven L. Tait*

Department of Chemistry, Indiana University, 800 E. Kirkwood Ave., Bloomington, Indiana 47405, United States

Supporting Information

ABSTRACT: The formation and stabilization of well-defined transition-metal single sites at surfaces may open new routes to achieve higher selectivity in heterogeneous catalysts. Organic ligand coordination to produce a well-defined oxidation state in weakly reducing metal sites at surfaces, desirable for selective catalysis, has not been achieved. Here, we address this using metallic platinum interacting with a dipyridyl tetrazine ligand on a single crystal gold surface. X-ray photoelectron spectroscopy measurements demonstrate the metal–ligand redox activity and are paired with molecular-resolution scanning probe microscopy to elucidate the structure of the metal–organic network. Comparison to the redox-inactive diphenyl tetrazine ligand as a control experiment illustrates that the redox activity and molecular-level ordering at the surface rely on two key elements of the metal complexes: (i) bidentate binding sites providing a suitable square-planar coordination geometry when paired around each Pt, and (ii) redox-active functional groups to enable charge transfer to a well-defined Pt(II) oxidation state. Ligand-mediated control over the oxidation state and structure of single-site metal centers that are in contact with a metal surface may enable advances in higher selectivity for next generation heterogeneous catalysts.

Stabilization and chemical control of transition-metal centers is a critical problem in the advancement of heterogeneous catalysts to next-generation catalysts that exhibit high levels of selectivity, while maintaining strong activity and facile catalyst recycling. Supported metal nanoparticle catalysts typically suffer from having a wide range of metal sites with different coordination numbers and varying chemistry. The use of metal–organic complexes in surface catalysts is therefore of interest to create well-defined and highly regular single-site centers.[1] Here, we report the formation of single-site Pt(II) centers within tetrazine-coordinated chains on a reconstructed Au(100) surface. We demonstrate that these redox-assembled chains are stable to 150 °C, bringing them into a temperature range of high interest for moderate temperature reactions, made feasible by lowering reaction temperatures by better catalyst control. They also serve as easily tuned model systems for exploring the chemistry of single-site transition metals that hold potential for future applications in tandem catalysts and development into a zeolite or other highly stable support structure.

On-surface coordination with small organic ligands is an active field of study that has been primarily devoted to the structural tuning of 2D metal–organic frameworks[2−7] or 1D chains[8−11] at surfaces by synthetic design of the ligands, but only rarely has insight into the metal oxidation state been obtained.[12−15] Access to new classes of ligands, many of which are weakly oxidizing,[16,17] is needed to develop opportunities for the catalytic functionalization of surfaces. Most studies of metal center assembly at surfaces have relied on readily reduced ligands, e.g., terephthalic acid,[14,18] tetracyanoquinodimethane,[15,19] and porphyrins.[20−22] Weakly oxidizing ligands, frequently utilized in solution-based metal complexes,[16,17] have been little studied at surfaces.[13,23] Weakly reducing metals, such as platinum,[24] have important applications in catalysis for carbophilic activation,[25−27] oxygen reduction,[28] and other reactions in solution-phase systems but have not been studied in the on-surface assembly of metal coordination networks.

We have developed a protocol to create single-site Pt(II) species (Figure 1) by on-surface, redox-active assembly under ultrahigh-vacuum conditions using dipyridyltetrazine (**1**, Scheme 1) and metallic Pt on the Au(100) surface. Tetrazines are the most electron-deficient aromatic ligands with room temperature stability[29] and have numerous applications in solution chemistry due to their coordination capabilities[16] and potential as bridging ligands for electronic coupling.[30] The redox chemistry in this system is not unlike that observed in metal–porphyrin complexation at surfaces.[20−22] Here, we utilize scanning tunneling microscopy (STM), noncontact atomic force microscopy (NC-AFM), and X-ray photoelectron spectroscopy (XPS) to provide insight into the on-surface redox chemistry leading to a highly organized adsorbate structure with well-defined single-site Pt(II) centers. We illustrate that the redox activity and molecular-level ordering at the surface rely on two key elements of the metal complexes: (i) binding pockets providing a nearly square-planar coordination geometry and (ii) redox-active subunits to enable charge transfer within the adsorbate layer.[31]

Ligand **1** and Pt were sequentially vapor deposited (in either order) on the Au(100) surface to form highly regular one-dimensional (1D) coordination chains of $(\mathbf{1}^{2-}\text{-}Pt^{2+})_n$. In order to develop a clear understanding of the molecular structure, we have imaged the chains by both STM and NC-AFM, which each provide single molecule resolution of the resulting surface structures. We note that the Au(100) surface undergoes a

Received: May 14, 2014
Published: June 24, 2014

dx.doi.org/10.1021/ja504850f | J. Am. Chem. Soc. 2014, 136, 9862–9865

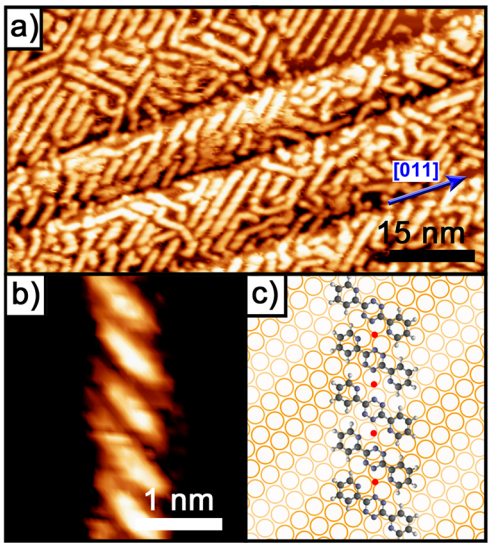

Figure 1. STM and AFM images of the **1**-Pt chains on the reconstructed Au(100) surface, annealed at 170 °C for 14 h, yielding a **1**:Pt ratio of 1 in the annealed surface structure. (a) STM wide scan image, with the [011] direction of the Au surface shown by the blue arrow. (b) NC-AFM molecular-resolution image of part of one chain. (c) Schematic model of the chains on the hexagonally reconstructed Au(100).

Scheme 1. Dipyridyl Tetrazine (1) and Diphenyl Tetrazine (2) Ligands Used in This Study and the $(1^{2-}\text{-}Pt^{2+})_n$ Polymer

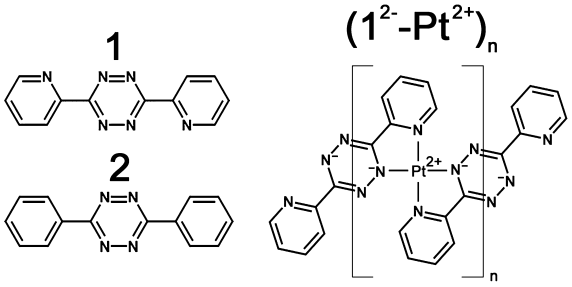

spontaneous reconstruction at the conditions used in this study, which leads to the appearance of straight rows in some of the scanning probe images. The reconstruction has been characterized generally as a quasi-hexagonal c(26 × 68),[32,33] although other structures may exist.[34]

The Pt sites are not clearly resolved in the STM images. NC-AFM images were also acquired in an attempt to resolve the Pt sites. The absence of single metal atom appearance in scanning probe images has been observed in other systems[35] and is generally understood to be related to a mismatch in the local density of electronic states and the small size of the metal dication. In spite of this, we have several pieces of experimental evidence that point to the complexation of Pt(II) centers with the tetrazine ligands through an on-surface redox process.

First, the observed surface morphology of 1D chains (Figure 1) is markedly different from the single component growth of either Pt or **1**. STM images of the Au(100) surface after vapor deposition of Pt (Figure 2c) show rectangular, nanometer-scale islands on the surface, which are elongated in the direction of the Au reconstruction rows, visible in the STM images. The measured height of the islands relative to the Au surface is only 2.3 ± 0.3 Å (Figure S5), indicating single atomic layer island height,[36] i.e., initial stages of layer-by-layer growth.[37] The

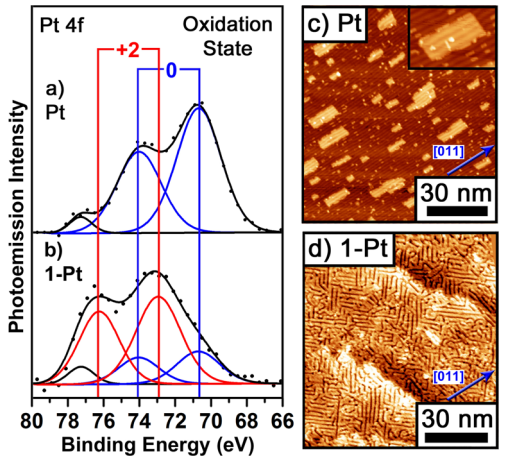

Figure 2. Platinum 4f XPS photoelectron peaks (a, b) and STM/AFM images (c, d) for Pt and **1**-Pt on the reconstructed Au(100) surface (spectral background subtraction applied). (a) Submonolayer quantity of Pt, annealed at 170 °C for 20 min. The gold surface does not oxidize Pt.[37] (b) Submonolayer quantity of Pt deposited onto a submonolayer quantity of **1**, followed by annealing at 150 °C for 20 min. Oxidation of Pt by ligand **1** is evidenced by the 2.2 eV chemical shift to higher binding energy[38] and referenced to Pt(II)-octaethylporphyrin on the same reconstructed gold surface (Pt $4f_{7/2}$ 72.7 eV, see SI). (c) Wide-scan STM image of the Pt islands after annealing at 170 °C for 15 min. (d) Wide-scan AFM image of the sample in (c), after addition of **1** and annealing again at 170 °C for 20 min.

dissolution of these 2D Pt islands is observed after **1** addition and annealing (Figures 2d and S7). With an excess of Pt (Pt:**1** ratio >1), both 1D **1**-Pt chains and 2D Pt islands are observed on the surface. The structure of pure **1** also differs significantly from that of **1**-Pt. Pure **1** forms ordered 2D molecular islands and a minority species of 1D chains (Figure S6); however, those chains are clearly distinct from the chains observed for **1**-Pt in that they are oriented parallel to the reconstruction rows, while the chains for **1**-Pt are oriented at 45° to the reconstruction rows (Figure S11). We note that the formation of the **1**-Pt chains does not seem to perturb the Au reconstruction, in contrast to an example of metal–porphyrin coupling to a surface reconstruction.[22]

Second, molecular resolution images of the 1D chains of **1**-Pt on the surface (Figure 1b) reveal a molecule–molecule distance of 6.5 ± 0.6 Å with the molecule axis at an angle of 55 ± 5° to the chain direction. The chains are running at 45 ± 5° to the reconstruction direction. Given this angle and molecule spacing, a model can be constructed (Figure 1c), which is *not* consistent with the chains being a packing of only **1**. Rather, a **1**-Pt chain provides an excellent match to the STM results, where tetrazine/pyridyl binding pockets form to provide a nearly square-planar coordination geometry around the Pt centers, the favored geometry for Pt(II). The Pt–N bond lengths in this structure are about 2.0–2.5 Å, consistent with expected bond lengths from inorganic complexes.[39,40]

Third, XPS measurements of the Pt 4f core level show a distinct chemical shift compared to metallic Pt islands on the same Au(100) surface (Figure 2a,b). This binding energy shift clearly indicates oxidation of the metal, which is anticipated upon complexation with the electron accepting tetrazine ligands.

Fourth, the stability of **1** against thermal desorption is markedly increased in the presence of Pt. XPS measurements

dx.doi.org/10.1021/ja504850f | J. Am. Chem. Soc. 2014, 136, 9862–9865

were made to quantify the coverage of **1** on the Au(100) surface before and after annealing treatment at 170 °C. When the **1** molecule is on the surface by itself, complete desorption is observed after this annealing treatment (Figure 3a,b).

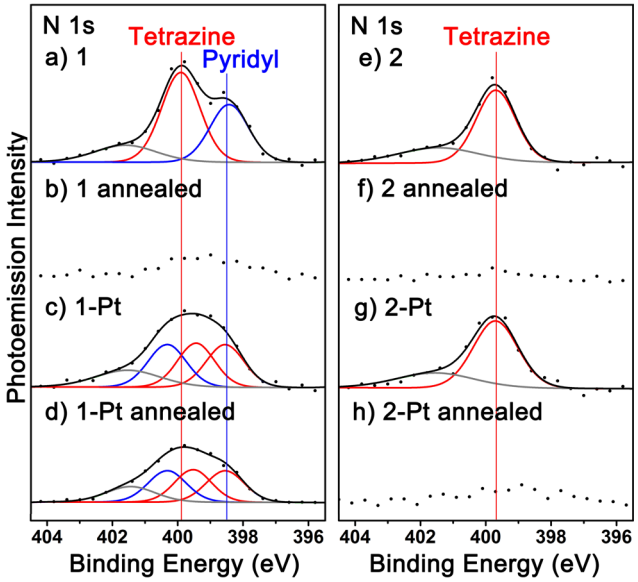

Figure 3. Nitrogen 1s XPS photoelectron peaks for **1** and **2** on the reconstructed Au(100) surface, in their pure form and after addition of Pt, before and after annealing. For each ligand species XP spectra are shown for the pure ligand before annealing (a, e) and after annealing at 170 °C for 10 min (b, f). Both **1** and **2** desorb after the annealing treatment in the absence of Pt. Spectra are also shown for the ligands after Pt addition, before annealing (c, g) and after annealing at 170 °C for 10 min (d, h). The $(\mathbf{1}^{2-}\text{-}Pt^{2+})_n$ polymer is stable against desorption with annealing, while **2** desorbs even with Pt.

However, in the presence of Pt, no significant desorption occurs (Figure 3c,d), indicating a strong interaction between Pt and **1**. The annealed **1**-Pt structure contains a 1:1 ratio of **1**:Pt, as confirmed by XPS. High-temperature STM experiments were conducted at 150 °C, and it was found that the chains could be clearly imaged at this elevated temperature, demonstrating excellent thermal stability (Figure 4). This stability is an indication of the strong redox coupling in the system and may be of interest in future applications of this and related transition-metal single site systems.

Fifth, XPS analysis of **1** in the **1**-Pt complexes shows a significant spectroscopic change (Figures 3a-3d), indicating an alteration in the chemical state of the ligand corresponding to the redox assembly. A monolayer of **1** on the Au(100) surface (Figure 3a) shows two N 1s features at energies of 399.8 and 398.3 eV, which correspond to the tetrazine and pyridyl N, respectively, and appear in the XP spectra in the 2:1 area ratio anticipated from the molecule structure. The N 1s features are the same as for **1** in its neutral, bulk form (Figure S1). Upon redox assembly with Pt, XPS measurement of N 1s features shows a significant change (Figure 3a–d), which can be interpreted by considering the two electrons acquired by the tetrazine, as expected from other examples of metal oxidation by tetrazine.[16] The degeneracy of the N 1s binding energy for the four tetrazine N atoms is lost; two of these N atoms are in close contact with the Pt, i.e., directly involved in the bidentate binding. It is expected that in such a binding geometry, the charge accepted by the tetrazine ligand would be concentrated

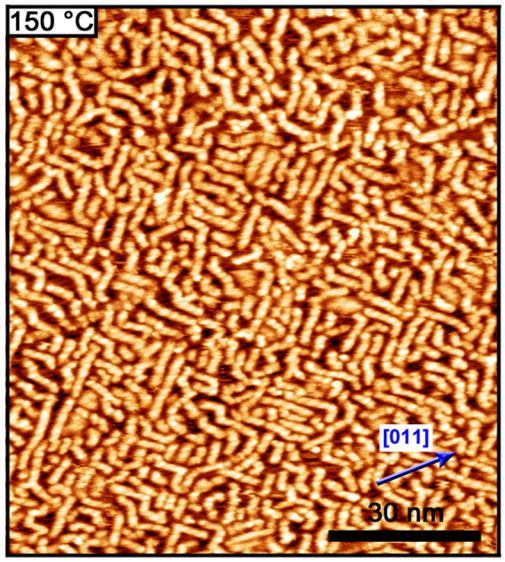

Figure 4. High-temperature STM image, acquired at a sample temperature of 150 °C, of the thermally stable 1D $(\mathbf{1}^{2-}\text{-}Pt^{2+})_n$ chains on the reconstructed Au(100) surface. The structure does not change over long time periods (see Figure S13).

around the two N atoms closest to the Pt(II) site, which would thus exhibit a strong affinity for the Pt dication. Thus, we fit the resulting N 1s spectrum (Figure 3c,d) with three components locked in a 1:1:1 ratio (see Supporting Information). XPS and STM did not resolve distinct features for the chain-terminating ligands, but one electron reduction is possible.[16]

The N 1s chemical shifts with Pt complexation, relative to the uncomplexed ligand, could thus be interpreted as either the tetrazine splitting into peaks at lower and higher BE and an unshifted pyridyl feature or the tetrazine splitting into two peaks that are each shifted to lower BE relative to the uncomplexed peak and the pyridyl component shifting to higher BE. The second interpretation agrees best with the bidentate arrangement observed by STM and NC-AFM and with prior XPS studies. N 1s chemical shifts to higher BE (>1 eV) are expected for the binding of neutral pyridines to transition-metal dications,[41,42] while the tetrazine is expected to shift to lower N 1s BE upon reduction.[43]

The importance of the square-planar coordination geometry in these single site Pt(II) complexes at a metal surface is confirmed by experiments combining Pt with ligand **2**, which contains the electron-accepting tetrazine group but lacks the pyridyl nitrogen atoms that are required for bidentate binding. In this case we do not observe any ordered assembly in the STM images (Figure S15), the Pt remains in a metallic (charge neutral) state (Figure S3), and the ligand desorbs with annealing (Figure 3h). The lack of a stable binding site and a clear square-planar coordination geometry seems to negate the potential for oxidation by the tetrazine in this case.

Based on the evidence in these experiments, we conclude that **1** is able to bind and stabilize the Pt as a +2 cationic species in 1D coordination chains of $(\mathbf{1}^{2-}\text{-}Pt^{2+})_n$. This behavior for a weakly oxidizing ligand and weakly reducing metal requires a well-designed combination of binding geometry and electron accepting character in the ligand. Ligand **1** provides a bidentate attachment to the Pt center; with two ligands attached to each Pt, a nearly square-planar coordination geometry is achieved, the geometry favored by Pt(II).[44] The tetrazine groups, which

dx.doi.org/10.1021/ja504850f | J. Am. Chem. Soc. 2014, 136, 9862–9865

are known to be better electron acceptors than pyridines,[17,29] aid the redox assembly.

These experiments indicate the need for a clear coordination geometry compatible with the desired metal oxidation state as well as an electron-accepting character of the ligands in order to achieve well-defined single-site transition-metal centers in nonzero oxidation states. These results are the starting point of many interesting questions related to the exploration of other metal ligand systems that may provide the ability to tune oxidation state and surface catalysis in a way that is familiar to inorganic chemists but has long been desired in surface heterogeneous catalysis.

■ ASSOCIATED CONTENT

Ⓢ Supporting Information

Experimental details, STM/AFM images, XPS data, and analysis of the metal−ligand structures. This material is available free of charge via the Internet at http://pubs.acs.org.

■ AUTHOR INFORMATION

Corresponding Author

tait@indiana.edu

Notes

The authors declare no competing financial interest.

■ ACKNOWLEDGMENTS

This work was supported by the Chemical Sciences, Geosciences and Biosciences Division, Office of Basic Energy Sciences, Office of Science, U.S. Department of Energy, Grant DE-FG02-12ER16351. We also thank Dr. Yaroslav Losovyj of the IU Nanocharacterization Facility.

■ REFERENCES

(1) Boscoboinik, J.; Kestell, J.; Garvey, M.; Weinert, M.; Tysoe, W. *Top Catal.* **2011**, *54*, 20.

(2) Vijayaraghavan, S.; Ecija, D.; Auwärter, W.; Joshi, S.; Seufert, K.; Drach, M.; Nieckarz, D.; Szabelski, P.; Aurisicchio, C.; Bonifazi, D.; Barth, J. V. *Chem.—Eur. J.* **2013**, *19*, 14143.

(3) Kley, C. S.; Čechal, J.; Kumagai, T.; Schramm, F.; Ruben, M.; Stepanow, S.; Kern, K. *J. Am. Chem. Soc.* **2012**, *134*, 6072.

(4) Barth, J. V. *Surf. Sci.* **2009**, *603*, 1533.

(5) Stepanow, S.; Lin, N.; Barth, J. V. *J. Phys.: Cond. Matter* **2008**, *20*, 184002.

(6) Yuan, Q. H.; Wan, L. J.; Jude, H.; Stang, P. J. *J. Am. Chem. Soc.* **2005**, *127*, 16279.

(7) Langner, A.; Tait, S. L.; Lin, N.; Rajadurai, C.; Ruben, M.; Kern, K. *Proc. Natl. Acad. Sci. U. S. A.* **2007**, *104*, 17927.

(8) Tait, S. L.; Langner, A.; Lin, N.; Stepanow, S.; Rajadurai, C.; Ruben, M.; Kern, K. *J. Phys. Chem. C* **2007**, *111*, 10982.

(9) Classen, T.; Fratesi, G.; Costantini, G.; Fabris, S.; Stadler, F. L.; Kim, C.; de Gironcoli, S.; Baroni, S.; Kern, K. *Angew. Chem., Int. Ed.* **2005**, *44*, 6142.

(10) Lin, T.; Shang, X. S.; Liu, P. N.; Lin, N. *J. Phys. Chem. C* **2013**, *117*, 23027.

(11) Shchyrba, A.; Nguyen, M.-T.; Wäckerlin, C.; Martens, S.; Nowakowska, S.; Ivas, T.; Roose, J.; Nijs, T.; Boz, S.; Schär, M.; Stöhr, M.; Pignedoli, C. A.; Thilgen, C.; Diederich, F.; Passerone, D.; Jung, T. A. *J. Am. Chem. Soc.* **2013**, *135*, 15270.

(12) Fabris, S.; Stepanow, S.; Lin, N.; Gambardella, P.; Dmitriev, A.; Honolka, J.; Baroni, S.; Kern, K. *Nano Lett.* **2011**, *11*, 5414.

(13) Yang, H. H.; Chu, Y. H.; Lu, C. I.; Yang, T. H.; Yang, K. J.; Kaun, C. C.; Hoffmann, G.; Lin, M. T. *ACS Nano* **2013**, *7*, 2814.

(14) Tait, S. L.; Wang, Y.; Costantini, G.; Lin, N.; Baraldi, A.; Esch, F.; Petaccia, L.; Lizzit, S.; Kern, K. *J. Am. Chem. Soc.* **2008**, *130*, 2108.

(15) Shi, X. Q.; Lin, C. S.; Minot, C.; Tseng, T. C.; Tait, S. L.; Lin, N.; Zhang, R. Q.; Kern, K.; Cerdá, J. I.; Van Hove, M. A. *J. Phys. Chem. C* **2010**, *114*, 17197.

(16) Kaim, W. *Coord. Chem. Rev.* **2002**, *230*, 127.

(17) Connelly, N. G.; Geiger, W. E. *Chem. Rev.* **1996**, *96*, 877.

(18) Lingenfelder, M. A.; Spillmann, H.; Dmitriev, A.; Stepanow, S.; Lin, N.; Barth, J. V.; Kern, K. *Chem.—Eur. J.* **2004**, *10*, 1913.

(19) Abdurakhmanova, N.; Floris, A.; Tseng, T. C.; Comisso, A.; Stepanow, S.; De Vita, A.; Kern, K. *Nat. Commun.* **2012**, *3*, 940.

(20) Diller, K.; Klappenberger, F.; Marschall, M.; Hermann, K.; Nefedov, A.; Wöll, C.; Barth, J. V. *J. Chem. Phys.* **2012**, *136*, 014705.

(21) Li, Y.; Xiao, J.; Shubina, T. E.; Chen, M.; Shi, Z.; Schmid, M.; Steinrück, H. P.; Gottfried, J. M.; Lin, N. *J. Am. Chem. Soc.* **2012**, *134*, 6401.

(22) Nowakowski, J.; Wäckerlin, C.; Girovsky, J.; Siewert, D.; Jung, T. A.; Ballav, N. *Chem. Commun.* **2013**, *49*, 2347.

(23) Álvarez, L.; Peláez, S.; Caillard, R.; Serena, P. A.; Martín-Gago, J. A.; Méndez, J. *Nanotechnology* **2010**, *21*, 305073.

(24) Bard, A. J.; Faulkner, L. R. *Electrochemical Methods: Fundamentals and Applications*; Wiley: New York, 1980.

(25) Periana, R. A.; Taube, D. J.; Gamble, S.; Taube, H.; Satoh, T.; Fujii, H. *Science* **1998**, *280*, 560.

(26) Lersch, M.; Tilset, M. *Chem. Rev.* **2005**, *105*, 2471.

(27) Fürstner, A.; Davies, P. W. *Angew. Chem., Int. Ed.* **2007**, *46*, 3410.

(28) Liang, C. C.; Juliard, A. L. *Nature* **1965**, *207*, 629.

(29) Clavier, G.; Audebert, P. *Chem. Rev.* **2010**, *110*, 3299.

(30) Castro, M. A.; Roitberg, A. E.; Cukiernik, F. D. *J. Chem. Theory Comput.* **2013**, *9*, 2609.

(31) Wäckerlin, C.; Iacovita, C.; Chylarecka, D.; Fesser, P.; Jung, T. A.; Ballav, N. *Chem. Commun.* **2011**, *47*, 9146.

(32) Vanhove, M. A.; Koestner, R. J.; Stair, P. C.; Biberian, J. P.; Kesmodel, L. L.; Bartos, I.; Somorjai, G. A. *Surf. Sci.* **1981**, *103*, 189.

(33) Vanhove, M. A.; Koestner, R. J.; Stair, P. C.; Biberian, J. P.; Kesmodel, L. L.; Bartos, I.; Somorjai, G. A. *Surf. Sci.* **1981**, *103*, 218.

(34) Binnig, G. K.; Rohrer, H.; Gerber, C.; Stoll, E. *Surf. Sci.* **1984**, *144*, 321.

(35) Ohshiro, T.; Ito, T.; Bühlmann, P.; Umezawa, Y. *Anal. Chem.* **2001**, *73*, 878.

(36) Furuya, N.; Ichinose, M.; Shibata, M. *J. Electroanal. Chem.* **1999**, *460*, 251.

(37) Michel, E. G.; Asensio, M. C.; Ferrer, S. *Surf. Sci.* **1988**, *198*, L365.

(38) Belogorokhov, A. I.; Bozhko, S. I.; Chaika, A. N.; Ionov, A. M.; Trophimov, S. A.; Rumiantseva, V. D.; Vyalikh, D. *Appl. Phys. A: Mater.* **2009**, *94*, 473.

(39) Rasmussen, P. G.; Anderson, J. E.; Bayón, J. C. *Inorg. Chim. Acta* **1984**, *87*, 159.

(40) Kircher, P.; Huttner, G.; Heinze, K.; Schiemenz, B.; Zsolnai, L.; Büchner, M.; Driess, A. *Eur. J. Inorg. Chem.* **1998**, *1998*, 703.

(41) Poppenberg, J.; Richter, S.; Darlatt, E.; Traulsen, C. H. H.; Min, H.; Unger, W. E. S.; Schalley, C. A. *Surf. Sci.* **2012**, *606*, 367.

(42) Gao, S. Y.; Huang, Y. B.; Cao, M. N.; Liu, T. F.; Cao, R. *J. Mater. Chem.* **2011**, *21*, 16467.

(43) Tseng, T. C.; Urban, C.; Wang, Y.; Otero, R.; Tait, S. L.; Alcami, M.; Ecija, D.; Trelka, M.; Gallego, J. M.; Lin, N.; Konuma, M.; Starke, U.; Nefedov, A.; Langner, A.; Woll, C.; Herranz, M. A.; Martin, F.; Martin, N.; Kern, K.; Miranda, R. *Nat. Chem.* **2010**, *2*, 374.

(44) Janes, R.; Moore, E. *Metal-ligand Bonding*; Royal Society of Chemistry: Cambridge, 2004.